Science Forum (Journal of Pure and Applied Sciences)

Journal Homepage: https://atbuscienceforum.com.ng/index.php/jpas

Velocity-Temperature Conversion in the Oceanic Lithosphere: Investigating Thermal Structure and Evolution Along the African Margins

Usman Yahaya Yaro*, Mustapha Aliyu, Nuru Abdullahi Nabage, Fatima Saidu
Department of Applied Geology, ATBU Bauchi

Abstract
This study investigates the relationship between seismic velocity and temperature in the lithosphere by utilizing high-resolution shear wave velocity models, cooling models, and heat flow data. The velocity models used in this study, primarily derived from Fishwick (2010), provide a detailed seismic tomography framework for analysing lithospheric temperature distribution. Comparisons were made with global models such as Schaeffer et al. (2013) and Kustowski et al. (2008) to assess model reliability and resolution differences. By applying both half-space and plate cooling models, the study estimates lithospheric thickness, thermal uplift, and subsidence patterns. Velocity-to-temperature conversion was conducted using a statistical approach as well as the empirical parameterization of Priestley & McKenzie (2006). Results indicate that the half-space cooling model predicts a continuously cooling lithosphere, while the plate model shows thermal equilibrium at older ages. Temperature estimates from shear wave velocities range from 375°C to 1746°C using the half-space model, and from 598°C to 1580°C using the plate model. The empirical parameterization by Priestley & McKenzie (2006) predicted lower temperatures, ranging from 140°C to 1280°C, and demonstrated better correlation with observed heat flow data. Temperature difference maps highlight slow velocity anomalies beneath the ocean ridge, Cape Verde, and Canary Islands, corresponding to regions of high thermal anomalies. Gravity data analysis reveals that faster seismic velocities coincide with negative free-air gravity anomalies and lower temperature deviations, while slower seismic velocities align with intermediate gravity anomalies and higher thermal deviations. These findings provide a refined understanding of lithospheric cooling patterns and contribute to geodynamic studies, petroleum exploration, and the assessment of regional thermal models. The study underscores the importance of integrating seismic, thermal, and gravity data for improved lithospheric characterization and highlights the need for expanding the analysis to the eastern margin of Africa and the Indian Ocean for a comprehensive regional assessment.

Keywords
Velocity-Temperature Conversion,
Oceanic Lithosphere,
Thermal Structure,
African Margins,

Corresponding Author: Usman Yahaya Yaro, *Department of Applied Geology, ATBU Bauchi.*

Introduction

The emergence of plate tectonic theory in 1915 and its subsequent world-wide acceptance in the 1950's (Wegener, 1966), revolutionised the science of geology. Generally, the theory refers to the movement and interaction between lithospheric plates at plate boundaries which are responsible for geologic events such as earthquakes, volcanism and mountain building. This new model was a combination of two previous theories, continental drift and sea-floor spreading, both of which were based on the lateral movements of the earth's continents and oceans relative to each other.

As this fundamental theory advances, mathematical cooling models (McKenzie, 1967; Turcotte and Oxburgh, 1967; Lister, 1974; Parsons and Sclater, 1977) described the thermal structure of oceanic lithosphere. The simple structure and evolution of oceanic plates, provides a perfect situation for the application of thermal models to plate tectonics. The separation of two lithospheric plates at mid-oceanic ridges, results in the ascension of hot mantle materials, which subsequently cools by conductive heat loss (Lister, 1974; Parsons and Sclater, 1977), and contracts. Consequently, this thermal contraction increases the mean density of the lithosphere, causing it to subside as it shifts away from the ridge. Observations of oceanic plates shows that away from the ocean ridges, there is a relationship between decreasing heat flow and increasing sea floor age (Fig. 1). Surface heat flow and ocean depths have been the principal observables on thermal cooling models and both have been used to map the thickness of oceanic lithosphere.

The most used models for describing the thermal structure of oceanic lithosphere are the half - space cooling model proposed by Turcotte and Oxburgh, (1967) and the plate cooling model originally proposed by McKenzie, (1967). The half – space cooling model assumes that the lithosphere will continue to cool and increase in thickness infinitely with increasing age. However, following the realisation that ocean depth flattens at older ages, McKenzie (1967) proposed the cooling plate model and impose a constant temperature T_m beneath the plate. This constant basal temperature limits the old lithosphere from growing by attaining a constant thickness. Comparison of the models' predictions with observed data shows that the plate model provides a good fit to average data. Although, predictions by both models have been successful in explaining the evolution of oceanic lithosphere with age, debate is still ongoing and different researchers have attempted to vary the model parameters in order to have the best fit to data. Because each research uses different set of parameters, it is difficult to compare the models predictions directly. However, there is no particular model that fits every region as evolution of the

lithosphere is not the same globally (Faul and Jackson, 2005).

The primary aim of this work is to compare between the conductive cooling models of oceanic lithosphere and seismology by comparing predictions of deep (sub-Moho) thermal structure with seismic tomographic models. Thermal conversion of shear velocity would allow a direct comparison of the structure modelled in the tomography especially in conjunction with theoretical cooling models which explains the thermal evolution of the lithosphere. Studies of seismic tomography have shown that there are significant differences between the velocity structure of continents and oceans (Goes et al., 2005; Priestley and McKenzie, 2006). Velocity variations due to mineral compositional effects are secondary compared to thermal effects (Cammarano et al., 2003; Furlong et al., 1995). Therefore, estimating the thermal structure which is a major cause of the velocity anomalies and comparing it with predictions from the cooling models would give a much more detailed information of the inner structure. The initial focus of this work is on the oceanic lithosphere for the Western Margin of Africa (fig. 1). However, subsequently, there is need to expand the scope to Eastern margin as well as the Indian Ocean, in order, to assess the normal cooling pattern of oceanic lithosphere. Similarly, comparison of the cooling pattern of oceanic lithosphere for these regions may further the understanding of evolution of oceanic lithosphere.

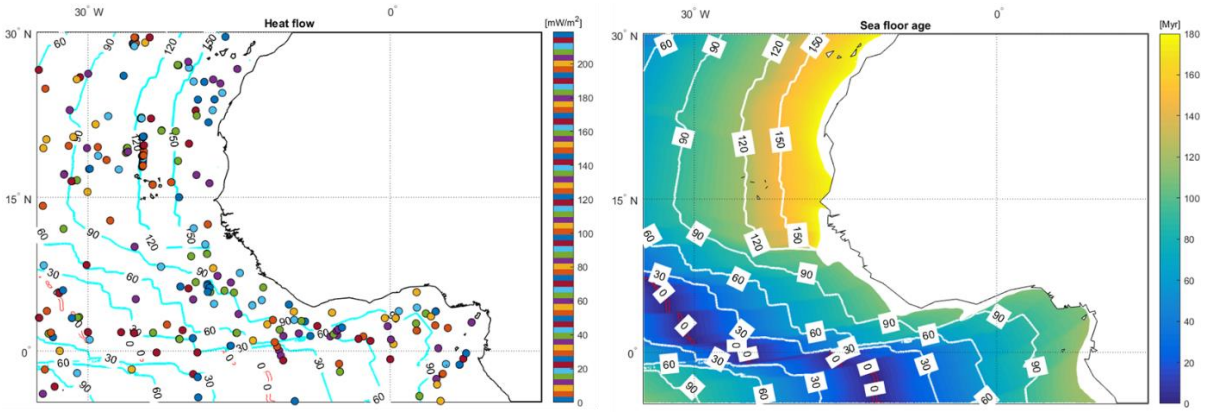

Figure 1: Left, surface heat flow map for the western coast of Africa. Purple contour lines indicate ocean age, red lines indicate the ocean ridge and small coloured circles indicate heat flow data points. Right, sea floor age map for the western coast of Africa. Heat flow data was taken from the global heat flow data base of the International Heat flow Commission (2006) & sea floor age was taken from Muller et al., (2008).

Review of Velocity – Temperature Conversion

Estimates of temperature within the lithospheric mantle using seismic data requires either mineral physics data or a parameterisation that assumes a thermal structure of the lithosphere. Previous studies conducted to infer temperatures from seismic velocities have been based on both forward and inverse modelling.

Yan et al., (1989) carried out research to estimate both temperature and composition in the upper mantle from P and S – wave tomographic models at a depth of 150 km using the experimental partial derivatives of elastic moduli of olivine with respect to changing temperature. The study further estimates a global surface heat flow map from the predicted temperature (based on shear wave velocities) anomalies and later compare the inferred global heat flow distribution with other published heat flow maps. Based on the results, there is an agreement between the observed and predicted heat flow anomalies at 150 km depth. Using a similar approach, Furlong et al., (1995) estimated the thermal structure of continental upper mantle from compressional and shear wave velocities. In contrast to Yan et al., (1989) the study jointly estimated the temperature and compositional variations from the tomographic models and interpreted the differences in the observed and predicted heat flow anomalies quantitatively. Rohm et al., (2000) estimated temperatures from shear wave velocity data for the continental upper mantle using laboratory measurements of density and elastic moduli for different mantle minerals. The study further compared the average heat flow measurements and S – wave velocity tomography models for different tectonic provinces and discover a negative correlation between the two data sets. Because of the strong negative correlation of heat flow measurements and S – wave velocity data between 60 km and 180 km depth, the study suggested that the velocity anomalies were mostly due to the influence of temperature.

Goes et al., (2000) performed a forward modelling of shear and compressional velocity data of Europe using parameters such as T, P and composition from different studies of mineral physics. The study used a regional tomographic model of shear wave velocity (adopted from Marquering and Sneider, 1996) and a global model of compressional wave velocity (adopted from Bijiwaard et al., 1988). The results of the study were used to assess how temperature, composition, anelasticity and partial melting affects both P and S – wave velocities. The study concluded that the velocity variations due to temperature anomalies are higher compared to compositional effects. Goes et al., (2002) conducted similar research by inverting P and S velocities using three different tomographic models of North American continent in order to map seismic temperatures. The thermal

structure was inferred using the method discussed by Goes et al., (2000). The velocity inversions for temperature were compared with temperature estimates from surface heat flow. The results from the study show that predicted temperatures for both P and S velocity inversions are in agreement with each other and consistent with those inferred from observed surface heat flow. The study further concluded that the velocity perturbations in the uppermost mantle are mainly due to temperature variations.

Cammarano et al., (2003) performed a forward modelling of mineral physics data in order to estimate the upper mantle temperatures and compositions from P and S – wave velocities and went further to assess the sensitivities of the synthetic model below 200 km depth. Additionally, the study highlights the uncertainties associated with forward modelling of mineral physics data into temperature, the dependence of the interpreted thermal anomalies on the reference model as well as the difficulties of distinguishing thermal and compositional anomalies. Goutorbe (2010) performed a forward modelling of seismic velocity data using the shear wave velocity model of Shapiro and Ritzwoller (2002) in order to infer the upper mantle temperatures. The forward modelling was done using parameters derived from mineral physics data. The study further considered fitting the seismic temperature, ocean depths and observed heat flow data with half – space, plate, and Chablis models. It was concluded that the model with a constant heat at the base of the plate (Chablis) provides the best to all the data sets. Goutorbe and Hillier (2013) estimated their seismic temperature using the same approach as in Goutorbe (2010), but improved the parameters of the three thermal models used by the latter by including a temperature and pressure dependent thermal conductivity, a temperature dependent heat capacity and initial condition of adiabatic decompression including melting.

Based on knowledge of the thermal structure of the lithosphere, Priestley and McKenzie (2006) joined the thermal models of the Pacific with P – T estimates from kimberlites in order to obtain an empirical relationship connecting velocity, temperature and pressure. The relationship was then used to convert the shear wave velocity data to temperature for the oceans and continents. Ritzwoller et al., (2004) performed a joint inversion of group velocities of Rayleigh and Love waves for the Pacific. The group velocities were then combined with phase velocities based on seismic and thermal parameterisation in order to produce a 3 D velocity model to 400 km. The temperature inversion was based on mineral physics data. The results from the inversions were then compared with predictions from half – space cooling model. The results from the comparison shows that the half – space cooling model

fits the data for ages younger than 70 Ma.

Description of the regional velocity model of the study area

The shear wave velocity model for this study was taken from the high resolution regional seismic tomography model of Fishwick (2010) for Africa using a global reference model AK135 (Kennett, 1995). The velocity model was created from a two-step inversion at interval of 25 km up to 400 km depth using output at 0.5^0 interval. In the first step, a waveform inversion of Rayleigh wave velocity data was used to create a 1 D velocity model for different time periods between 50 and 120 s for both fundamental and first four higher modes. The higher modes were used to enhance the vertical resolution of the surface wave data. The study utilized only sources that are confined to Africa and its proximity with a large path coverage of 11,900 (fig. 2). For each path (earthquake – receiver combination) a 1 D model was constructed. As a quality control, four starting models were run for each seismogram and only 3 out of 4 final models were required to give a reasonable solution in order, to be selected for the inversion. In the second step the 1 D model was averaged to produce a 2 D shear wave velocity structure.

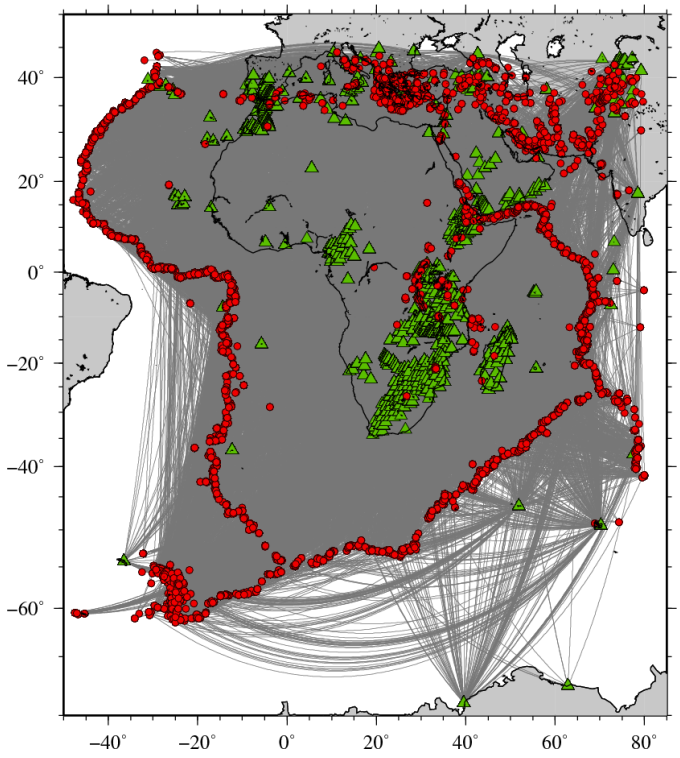

Figure 2: Full path coverage of source - receiver used for the tomography study (plot taken from Fishwick, 2010).

However, assessing uncertainties in depth resolution is challenging as each path average model contains different information in terms of frequency and higher mode content, leading to different depth resolution. Consequently, the vertical averaging / smearing cannot be assessed in the layer-by-layer inversion used in Fishwick (2010). Figure 3 shows the velocity perturbation map for the study area. The velocity map shows slow velocity anomalies beneath the ocean ridge located at the bottom – left part of the map and increasing fast velocity anomalies away from the ridge towards the continental margin. The slow velocity anomalies observed beneath the ocean ridge are due to the ascension of hot buoyant mantle materials and the fast anomalies are caused by increased cooling and thickening of the lithosphere away from the spreading axis. Other areas of slow anomalies shown by the map are also seen below the Cape Verde and Canary Islands. The slow anomalies are due to presence of hotspots beneath these Islands.

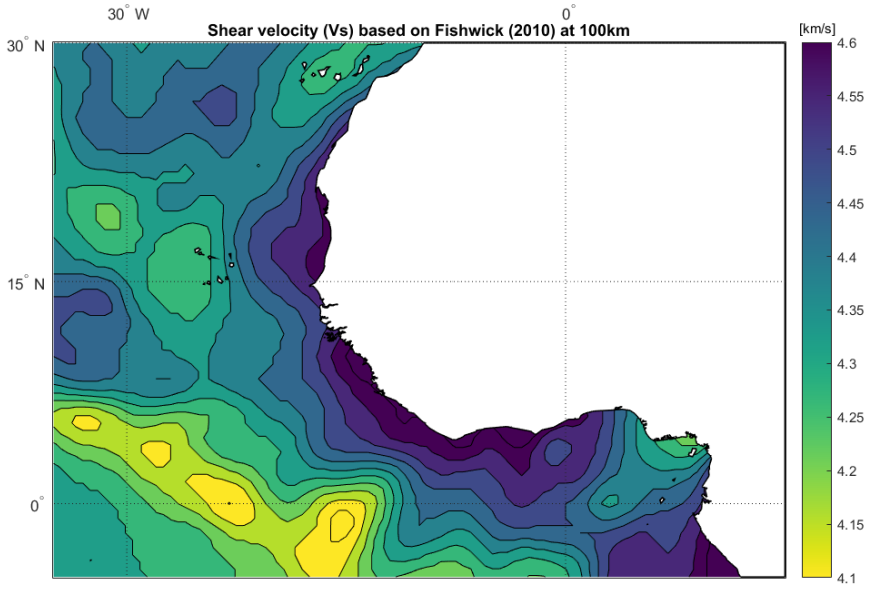

Figure 3: Seismic velocity anomalies at 100km depth. The S – wave velocity model is part of the regional model of Fishwick (2010) for the Western Coast of Africa.

Qualitative comparison of the regional velocity model with published global models for Western margin of Africa.

The shear wave velocity model for the study area taken from Fishwick (2010) (fig. 4, top) was compared with other published shear wave velocity models for the same area. Comparison of the Fishwick (2010) model with a published model (fig. 4; bottom, left) by Shaeffer et al., (2013) shows similarity in the velocity signatures both for regions of slow and fast velocities.

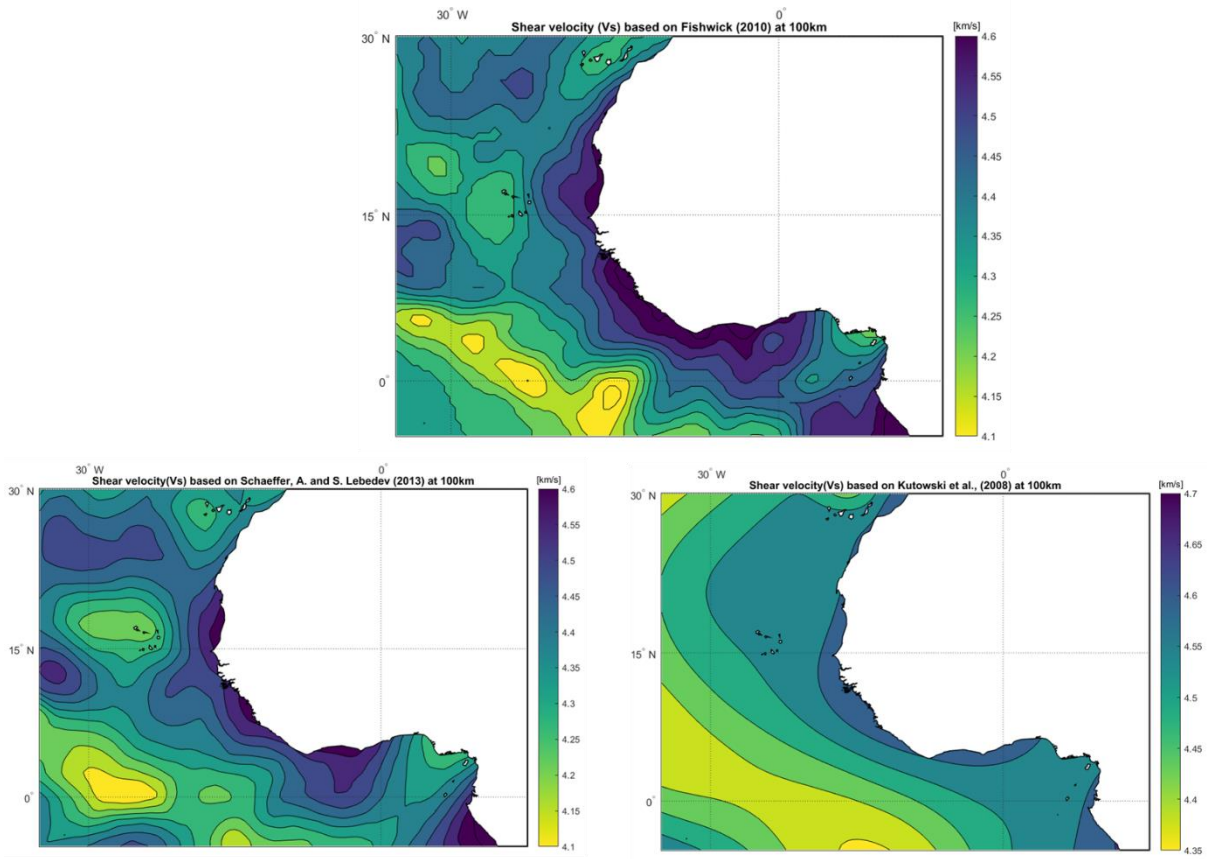

Figure 4: Comparison of regional shear wave velocity model and global models for the study area at 100 km depth.

For instance, in both models, the ocean ridge (located at the bottom – left of the map) shows a strong slow velocity signature. Additionally, the models reveal a strong fast velocity signature at the continental margins. However, the model of Shaeffer et al., (2013) shows lower velocities beneath the Cape Verde Island which is believed to have been underlain by hotspot. Similarly, the model of Fishwick (2010) reveal small scale structures beneath the ocean ridge as well as in the entire region. This is probably due to the fact that the velocity model of Shaeffer et al., (2013) is a global model with less dense sampling and lower resolution compared to the regional model of Fishwick (2010).

Further comparison of the two (Fishwick, 2010; Shaeffer et al., 2013) models with another global model (fig. 4; bottom, right) produced by Kutowski et al., (2008), shows that the model only reveals large scale features compared to the previous models discussed earlier. However, the model (Kutowski et al., 2008) shows smaller variation in velocity and hotter lithosphere beneath the ocean ridge.

Methodology

Temperature from shear wave velocity using statistical approach

The initial step for the velocity – temperature conversion was to establish a trend between the shear wave velocity data for the study area taken from the regional seismic tomography model of Fishwick (2010) and sea floor age data. The shear wave velocity data for the Western margin of Africa has sparse data coverage (0.5° x 0.5°) compared to the sea floor age data grids produced by Muller et al., (2008), which has grid resolution of 2 arc min. Therefore, the sea floor age data was stacked on the shear wave velocity (Vs) data.

Subsequently, the temperatures were estimated from the sea floor age, since the temperature structure of oceanic lithosphere depends on the sea floor age. A cross plot of shear wave velocity (Vs) and temperature for half-space cooling model using an adiabatic component (based on calculations from Faul and Jackson, 2005) and plate model (parameters are based on Hoggard et al., 2017) were obtained. Shear velocity - temperature cross plot for half – space model (fig. 5, left) at 100 km depth with best fitting polynom of degree 3, shows regions of high-density points towards the centre as well as at the south western edge of the plot (at ~1330 °C). Similar cross plot (fig. 5, right) for plate model with best fitting polynom of degree 1, shows a linear trend of increasing temperature with decreasing velocity as opposed to degree 3 polynom for half-space cooling model.

Following the scattered plots for the shear wave velocity against temperature, however, it was difficult to establish a good fit because of the concentration of data points skewing parallel to the temperature axis on the velocity – temperature cross plots. As a result, a statistical approach was devised in order to estimate the mean shear velocity for every 10 Ma interval. The shear wave velocity data was again interpolated on the seafloor age data. The grouped seafloor age data was plotted against the average shear wave velocity data for those ages (fig. 6). The seafloor age was later converted to temperature and an optimal fitting (i. e, the line that fit the mean values the best) was drawn on the temperature versus shear wave velocity plot for both half – space (fig. 7, left) and plate cooling models (fig. 7, right). The equations linking the shear wave velocity data and temperature at 100 km depth is given by equations 5.1 and 5.2 for the half – space and plate cooling models, respectively.

From these equations temperature maps were produced. Furthermore, the calculated temperatures for both half-space and plate cooling models had been subtracted from the estimated temperatures to obtain the temperature difference maps. Subsequently, these temperature deviations were compared with gravity anomalies. The misfit for this approach was estimated using equation 5.3 by calculating the sum of the absolute temperature differences between the model temperature

prediction and the observed temperature from the shear velocity.

$$T(V_s) = -1.5047 \times 10^3 V_s + 7.7241 \times 10^3 \quad 5.1$$

$$T(V_s) = -1.4443 \times 10^3 V_s + 7.4870 \times 10^3 \quad 5.2$$

$$Misfit = \sum \left| T_{model} - T(V_s) \right| \quad 5.3$$

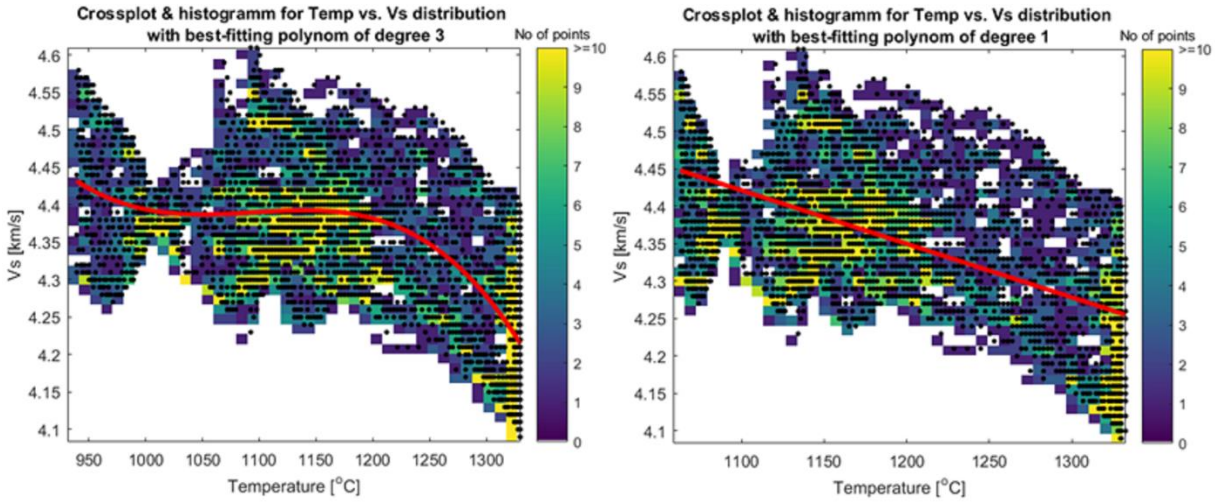

Figure 5: Cross plots and histogram of Temperature vs Shear wave velocity (Vs) distribution for (left)half-space cooling model (adiabatic component included) at 100 km depth with best fitting polynom of degree 3 and (right) plate cooling model with asymptotic depth of 130 km at 100 km depth with best fitting polynom of degree 1.

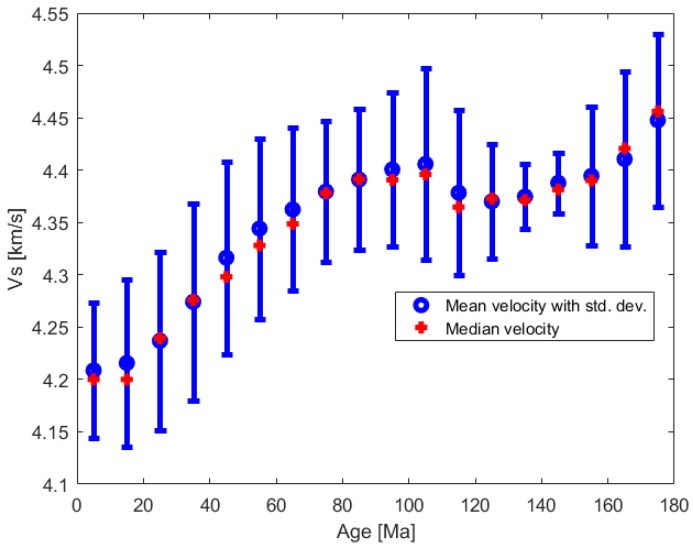

Figure 6: Shear velocity - age velocity relationship for the western margin of Africa.

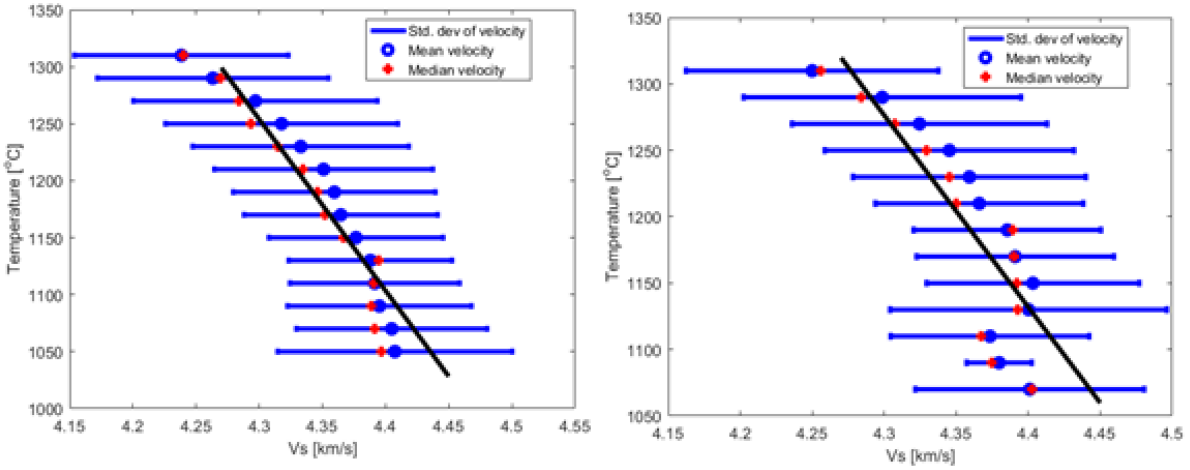

Figure 7: Temperature - shear wave velocity relationship for Western margin of Africa using (left) Half-space cooling model (adiabatic component included) and (right) plate model with asymptotic thickness (a) of 130 km and mantle potential temperature of 1330 °C at 100 km depth with best fitting polynom of degree 1.

Temperature from shear wave velocity based on Priestly and McKenzie (2006)'s empirical parameterization

Similar to the statistical approach described earlier which was purely based on simple empirical relationship between the shear wave velocity and temperature calculated from the seafloor age, as well as on the assumption that oceanic lithosphere has a simple structure, the Priestly and McKenzie (2006)'s empirical relationship for the oceans incorporates parameters suitable for combining tomographic velocities with constraints from plate cooling model. The equation linking the shear wave velocity (V_s) and temperature (T) is given by;

$$V_s = [1 + b_v(z - 50)] \times \left\{mT + c + Aexp\left[\frac{E + PV_a}{R(T + 273.15)}\right]\right\} \qquad 5.4$$

$$Where, b_v = 3.84 \times 10^{-4}\, Km^{-1}, m = -2.8 \times 10^{-1}\, ms^{-1}\, \oint, A = -1.8 \times 10^{16} ms^{-1}$$

$$E = 409 \times 10^{3} Jmol^{-1}, V_a = 10^{-6} m^3 mol^{-1}, R = 8.3145\, Jmol^{-1}K^{-1}, c = 4720\, ms^{-1}$$

$$z = depth, V_a = activation\ volume, E = activation\ energy, R = gas\ constant,$$

$$P = pressure = \rho gz, \rho = 3300\, kgm^{-3}, g = 9.81\, ms^{-2}.$$

The conversion of shear velocity to temperature using Priestley & McKenzie (2006)'s parameterisation began by calculating the theoretical shear velocity (V_S). At every 0.5°, V_S was modelled and equation 5.4 was used with a range of temperatures (0 – 1290 °C) at 10 °C interval. The theoretical velocity was further compared with the observed shear velocity in order to obtain the minimum difference between the two velocities. As a quality control, the temperature that generates the minimum misfit at each data point was used as the converted temperature (fig. 8). The misfit can be minimised by using a smaller step of temperatures.

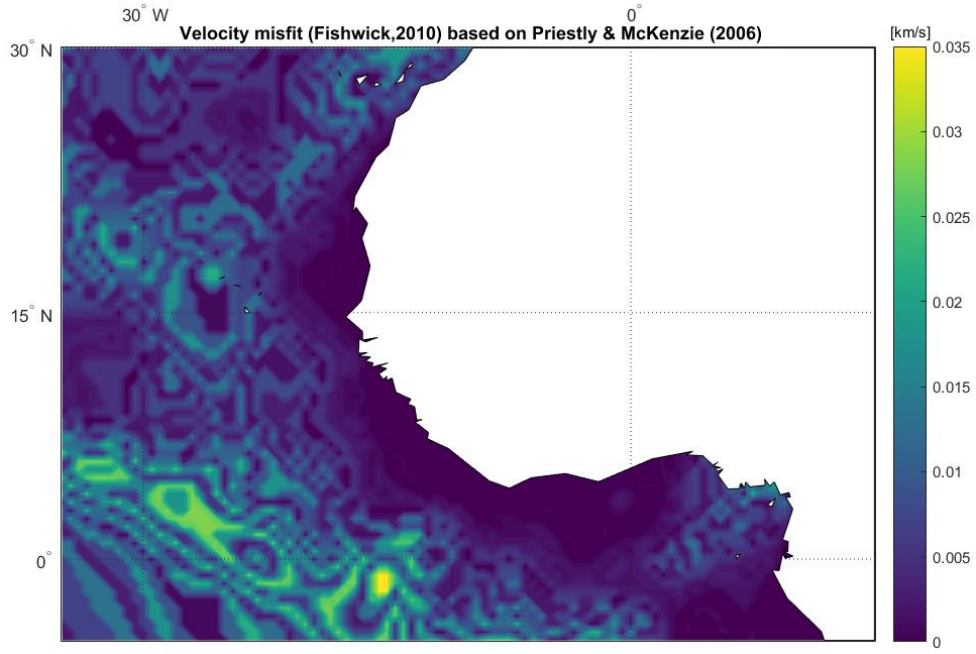

Figure 8: Velocity misfit map between observed velocity (Fishwick, 2010) and theoretical velocity (Priestley and McKenzie, 2006).

Gravity data

Gravity measurements can be used to infer whether an area is in isostatic balance. Therefore, if a region is isostatically stable there should be no additional or lack of mass above the compensation depth. The free – air anomaly includes the effects of all the mass variations that underlies the measurement point. In contrast, the Bouguer anomaly has had the effect due to mass of the topography removed. Therefore, the two can be used to investigate the stability and instability of tectonic regions. The gravity data used in producing the free-air (fig. 9) and bouguer gravity (fig. 10) anomaly maps is a satellite data taken from the International Centre for Global Earth Models (ICGEM). The advantage of using

a satellite data is that there is a full coverage compared to observed ground data. The model used was based on GOCO05s with about 7171 number of grid points and a grid step of $0.5^0 \times 0.5^0$ equivalent to the shear wave velocity model grid size. The model is based on a reference system WGS84 with a maximum degree of 65.

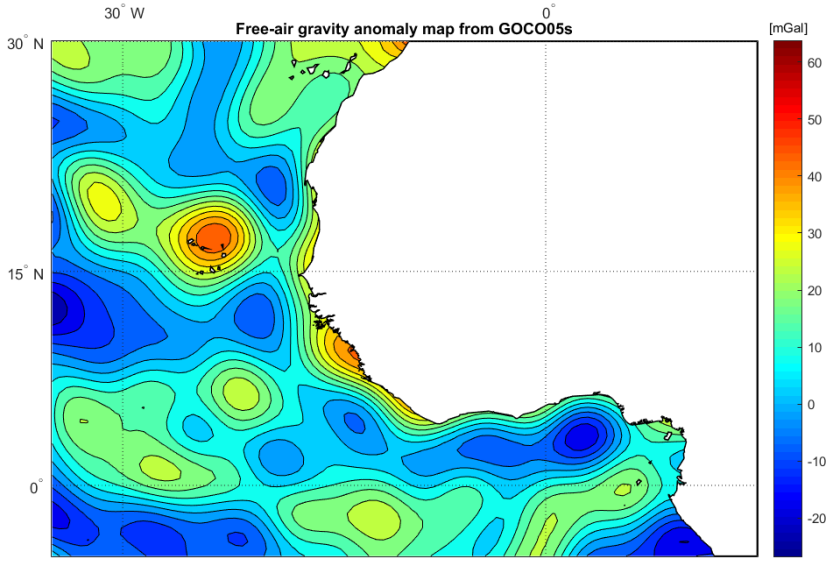

Figure 9: Free-air gravity anomaly map for the study area (adopted from GOCO05s).

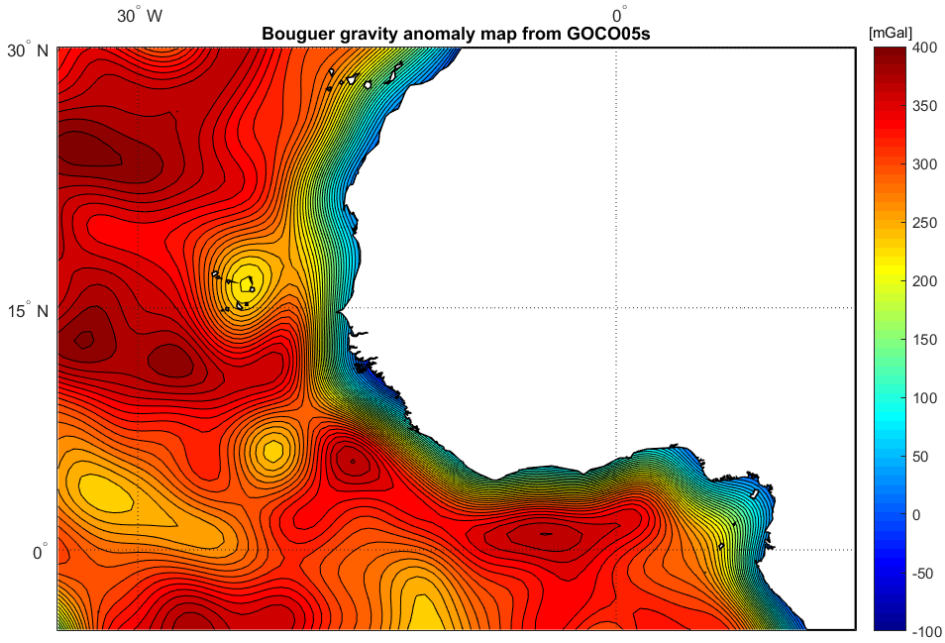

Figure 10: Bouguer gravity anomaly map for the study area (adopted from GOCO05s).

The gravity maps were smoothed using a small spherical harmonic of 65 so that only long wavelengths anomalies are enhanced. Based on these coordinates (latitude: 30^0 and -5^0 and longitude: 15^0 and -35^0), the gravity grids were imported to Matlab environment to produce gravity anomaly maps.

Results

Estimated temperatures from shear wave velocities

Using a mantle potential temperature of 1330 °C adapted from Hoggard et al., (2017), temperatures were estimated from shear wave velocity for plate cooling model (fig. 11) and half - space model (fig. 12) at 100 km depths respectively. Temperature estimates range from 375 °C to 1746 °C for conversion using half - space model and 598 °C to 1580 °C for plate model. These temperature ranges reflect predictions from continental margins to ocean ridges. The colder lithosphere observed away from the ridge axis for half – space cooling model is due to the fact that the model assumes continuous cooling for older ages. The misfits for conversion using plate model is 464 °C and using half – space model. Temperature estimates based on Priestley & McKenzie (2006)'s empirical parameterization (fig. 13) ranges from 140 °C to 1280 °C and a misfit between the observed and theoretical velocities are between 0.01 to 0.035 Km s^{-1}. The Priestley and McKenzie (2006)'s empirical parameterization predicted lower temperatures compared to half – space and plate cooling models.

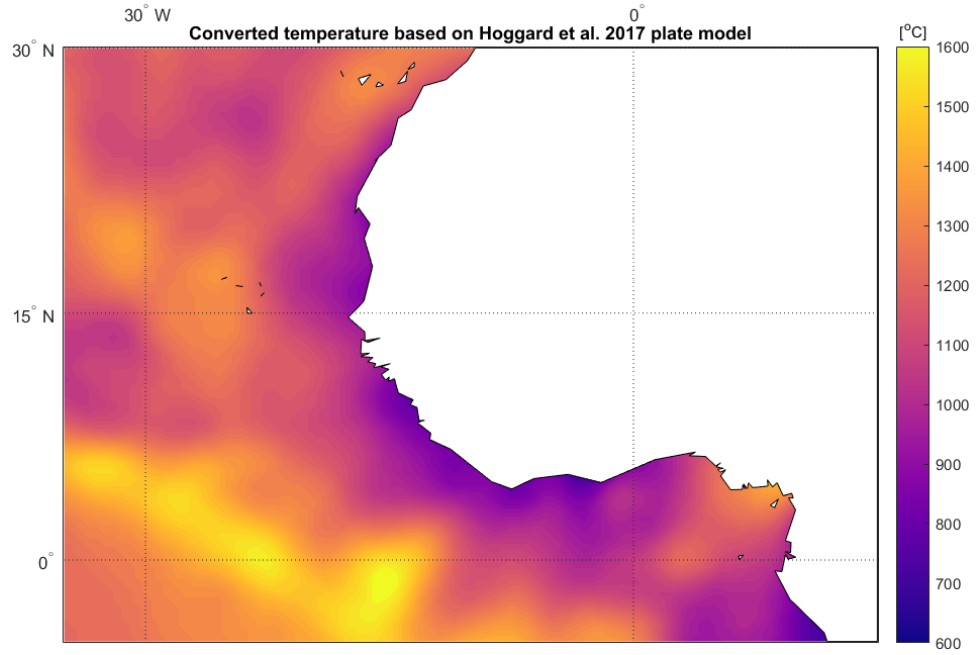

Figure 11: Estimated temperatures from shear wave velocities for plate model at 100 km depth with asymptotic thickness of 130 km and mantle potential temperature of 1330 °C.

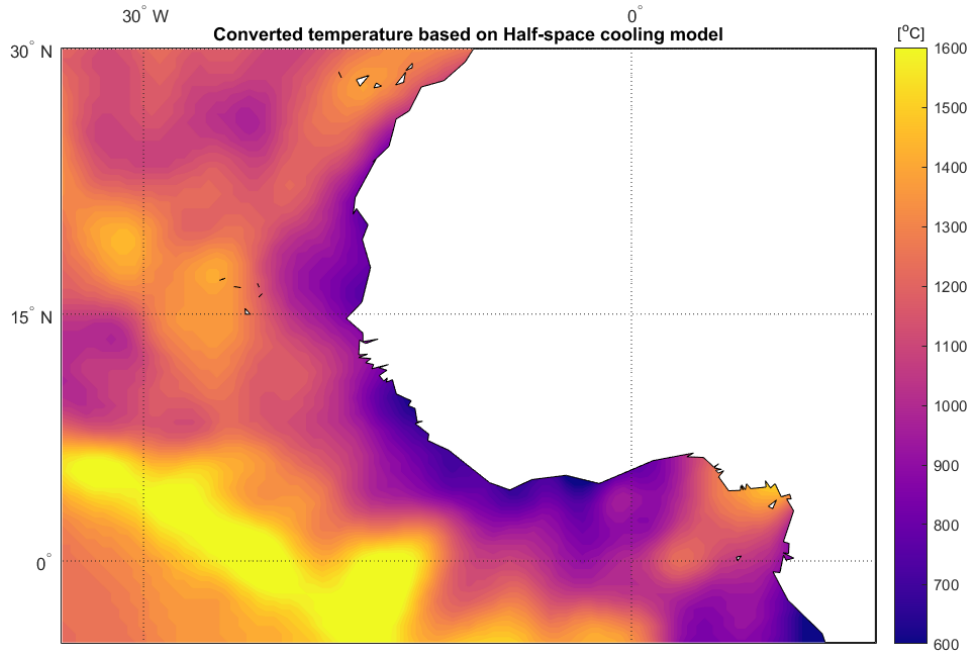

Figure 12: Estimated temperatures from shear wave velocities for Half-space cooling model (adiabatic component included) at 100 km depth. The adiabatic parameters were based on equation (2.2) using Tm = 1330 ^{0}C, Ts = 0 ^{0}C, Cp = 1350 JKg^{-1}K^{-1}, k = 8.04 x 10^{-7} m^{2}s^{-2} and αT = 2.9 x 10^{-5} K^{-1}.

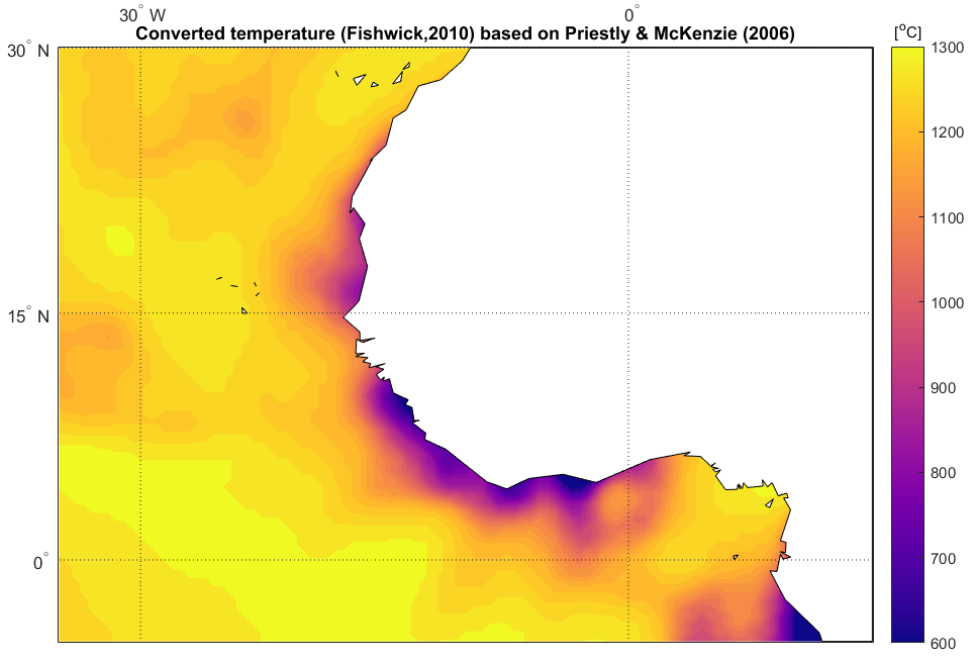

Figure 13: Estimated temperatures from shear wave velocities based on Priestly and McKenzie (2006)'s empirical parameterization at 100 km depth.

Figure 14, shows the variations of mean temperatures for the three models with age for 5 Ma interval. Accordingly, the models mean predictions shows a better correlation at ages greater than 45 Ma than at younger age. Based on Priestley & McKenzie (2006)'s parameterization the mean temperatures for 5 Ma interval are almost constant for all ages. The mean temperatures for the half – space and plate models have better correlation with each other than with Priestley & McKenzie (2006)'s parameterization. The half – space cooling model shows higher mean temperatures at younger age and lower mean temperatures at older age. The maximum mean temperatures for the model are 1513 °C for ages between 5 – 10 Ma and the minimum is 1014 °C for ages 175 – 180 Ma.

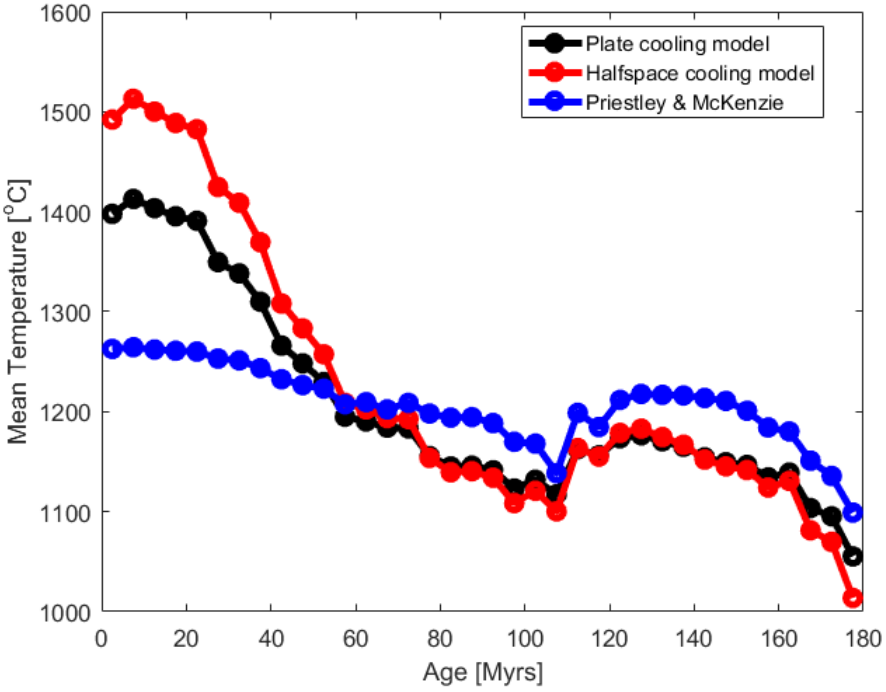

Figure 14: Variations of mean lithospheric temperatures with age for half - space, plate and Priestley & McKenzie (2006) models.

Temperature difference maps

The calculated temperatures for both half-space and plate cooling models have been subtracted from the estimated shear wave velocity temperatures. The difference between the seismic temperatures and the ones from plate cooling model gives temperature ranges between -448 °C and 392 °C (fig. 15). Similarly, temperature deviations from half-space cooling model ranges between -327 °C and 252 °C (fig. 16). In both maps, regions of higher/lower temperature difference anomalies coincide with portions where the estimated shear wave velocity

temperatures are higher/lower than the calculated temperatures for both half-space and plate cooling models. The two temperature difference maps have shown slow velocity anomalies beneath the ridge axis, Cape Verde and Canary Islands. These regions of slow velocities correspond to the tops of regions of low-density anomalies.

Temperature difference for plate model subtracted from Priestley & McKenzie (2006)'s empirical parameterization gives a minimum of -483 °C and a maximum of 182 °C (fig. 17). This shows that the plate model with parameters adapted from Hoggard et al., (2017) has higher temperatures than the ones used by Priestley & McKenzie (2006).

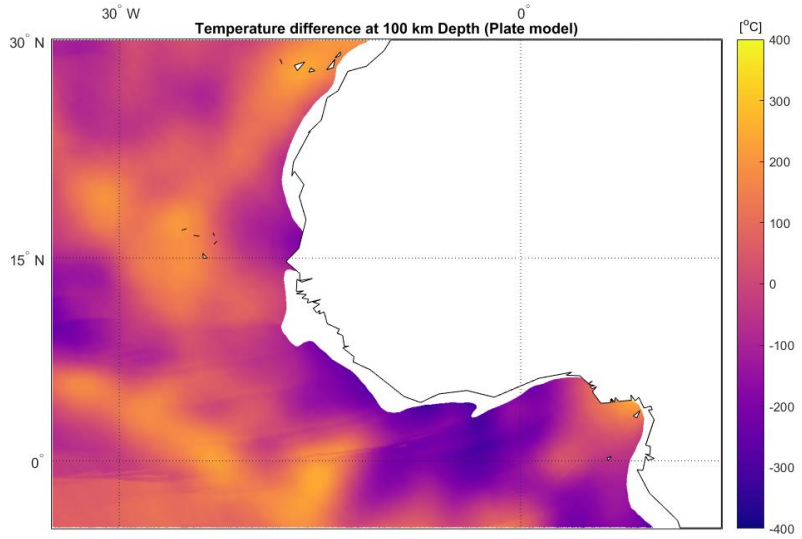

Figure 15: Temperature deviations for plate cooling model subtracted from converted temperature.

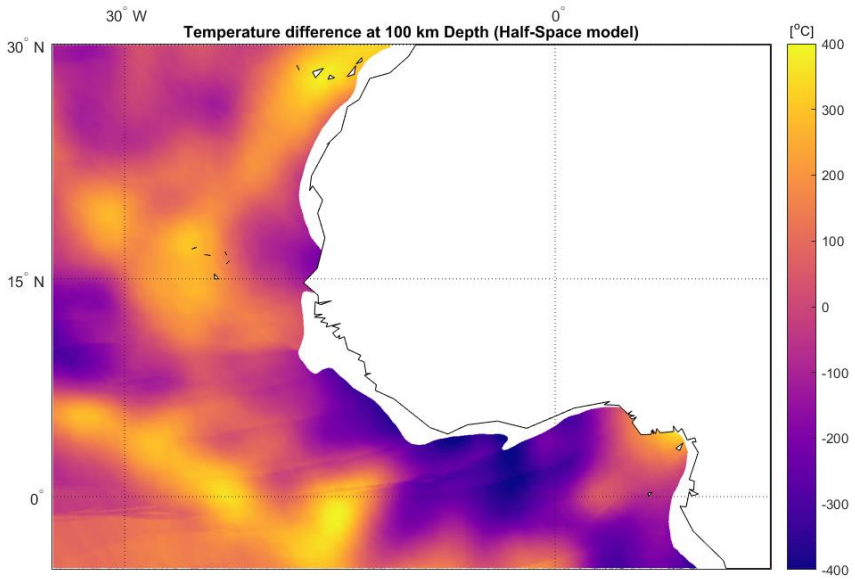

Figure 16: Temperature deviations for half-space cooling model subtracted from converted temperature.

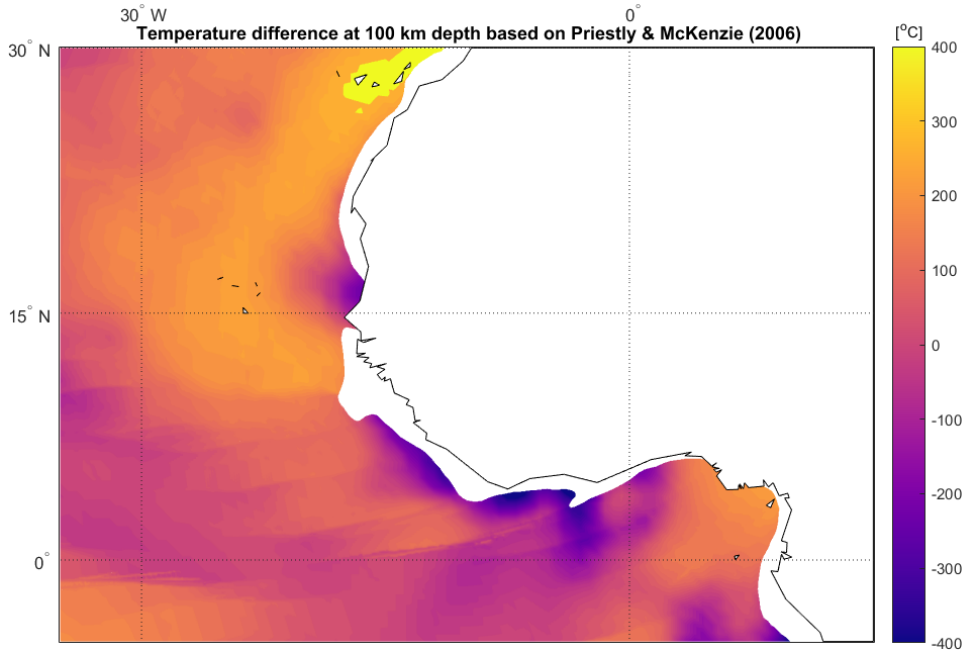

Figure 17: Temperature deviations for plate cooling model subtracted from converted temperature based on Priestley & Mckenzie (2006).

The free – air gravity anomaly values for the study area ranges from -27 mGal to +64 mGal and shows (fig. 9) regions of positive gravity anomalies on the Cape Verde Hotspots due to their high topography. The ocean ridge has intermediate anomalies (almost zero) indicating that they are isostatically stable. The small long wavelength positive anomalies near the ridge axis are as a result of higher elevation of the ridge. The gravity anomaly maps were compared with temperature difference maps as well as the velocity perturbations. Regions of faster shear wave velocities have negative free-air anomaly as well as lower temperature difference signatures. Similarly, areas of slow velocity anomalies are seen to coincide with intermediate free-air anomalies and higher temperature difference signatures. The bouguer gravity values ranges between -98 mGal to +396 mGal and the anomaly map (fig. 10) show areas of high, intermediate and low bouguer gravity anomalies. The high bouguer gravity anomalies match with regions of fast velocities as well as low temperature difference anomalies. Regions of intermediate bouguer gravity anomalies correlates well with areas of high temperature difference anomalies as well as slow velocity anomalies. Additionally, areas of negative bouguer gravity anomalies correlates with the continental margins.

Conclusion

- Using the knowledge of the thermal structure of the

lithosphere, this study has estimated temperatures at 100 km depths from shear speed model of Fishwick (2010) for the western coast of Africa.

- The velocity – temperature conversion was conducted using two approaches: firstly, a statistical method comparing velocities and predicted temperatures. Secondly, using the approach of Priestley & McKenzie (2006).
- Based on the statistical approach, the half – space cooling model predicted colder lithosphere away from the ridge and hotter lithosphere beneath the ridge in comparison to plate cooling model.
- The Priestley & McKenzie (2006)'s approach predicted lower temperatures both at the continental margin and beneath the ridge.
- The models mean temperature predictions for 5 Ma interval shows a better correlation for ages greater than 45 Ma than at younger age.
- In order, to assess the normal cooling of oceanic lithosphere, however, there is need to expand the scope of this study to eastern coast of Africa and the Indian Ocean.

References

Afonso, J.C., Fernandez, M., Ranalli, G., Griffin, W.L. and Connolly, J.A.D., 2008. Integrated geophysical-petrological modeling of the lithosphere and sublithospheric upper mantle: Methodology and applications. *Geochemistry, Geophysics, Geosystems*, *9*(5).

Anderson, D.L. and Regan, J., 1983. Upper mantle anisotropy and the oceanic lithosphere. *Geophysical research letters*, *10*(9), pp.841-844.

Artemieva, I.M., 2009. The continental lithosphere: reconciling thermal, seismic, and petrologic data. *Lithos*, *109*(1), pp.23-46.

Bown, J.W. and White, R.S., 1994. Variation with spreading rate of oceanic crustal thickness and geochemistry. *Earth and Planetary Science Letters*, *121*(3-4), pp.435-449.

Brown, C., 1994. Tectonic interpretation of regional conductivity anomalies. *Surveys in Geophysics*, *15*(2), pp.123-157.

Cammarano, F., Goes, S., Vacher, P. and Giardini, D., 2003. Inferring upper-mantle temperatures from seismic velocities. *Physics of the Earth and Planetary Interiors*, *138*(3), pp.197-222.

Cannat, M., Mevel, C., Maia, M., Deplus, C., Durand, C., Gente, P., Agrinier, P., Belarouchi, A., Dubuisson, G., Humler, E. and Reynolds, J., 1995. Thin crust, ultramafic exposures, and rugged faulting patterns at the Mid-Atlantic

Ridge (22–24 N). *Geology*, *23*(1), pp.49-52.

Carlson, R.L. and Johnson, H.P., 1994. On modeling the thermal evolution of the oceanic upper mantle: An assessment of the cooling plate model. *Journal of Geophysical Research: Solid Earth*, *99*(B2), pp.3201-3214.

Crosby, A.G., 2006. *Aspects of the relationship between topography and gravity on the Earth and Moon* (Doctoral dissertation, University of Cambridge).

Crosby, A.G., McKenzie, D. and Sclater, J.G., 2006. The relationship between depth, age and gravity in the oceans. *Geophysical Journal International*, *166*(2), pp.553-573.

Davies, G.F., 1988. Ocean bathymetry and mantle convection: 1. large-scale flow and hotspots. *Journal of Geophysical Research: Solid Earth*, *93*(B9), pp.10467-10480.

Davis, E.E. and Lister, C.R.B., 1974. Fundamentals of ridge crest topography. *Earth and Planetary Science Letters*, *21*(4), pp.405-413.

Debayle, E., Dubuffet, F. and Durand, S., 2016. An automatically updated S-wave model of the upper mantle and the depth extent of azimuthal anisotropy. *Geophysical Research Letters*, *43*(2), pp.674-682.

Debayle, E., Kennett, B. and Priestley, K., 2005. Global azimuthal seismic anisotropy and the unique plate-motion deformation of Australia. *Nature*, *433*(7025), pp.509-512.

Deen, T.J., Griffin, W.L., Begg, G., O'Reilly, S.Y., Natapov, L.M. and Hronsky, J., 2006. Thermal and compositional structure of the subcontinental lithospheric mantle: Derivation from shear wave seismic tomography. *Geochemistry, Geophysics, Geosystems*, *7*(7).

Doin, M.P. and Fleitout, L., 1996. Thermal evolution of the oceanic lithosphere: an alternative view. *Earth and Planetary Science Letters*, *142*(1-2), pp.121-136.

Faul, U.H. and Jackson, I., 2005. The seismological signature of temperature and grain size variations in the upper mantle. *Earth and Planetary Science Letters*, *234*(1), pp.119-134.

Fishwick, S., 2010. Surface wave tomography: imaging of the lithosphere–asthenosphere boundary beneath central and southern Africa? *Lithos*, *120*(1), pp.63-73.

Fishwick, S., 2006. Gradient maps: A tool in the interpretation of tomographic images. *Physics of the earth and planetary interiors*, *156*(1), pp.152-157.

Forsyth, D.W., 1977. The evolution of the upper mantle beneath mid-ocean ridges. *Tectonophysics*, *38*(1-2), pp.89-118.

Furlong, K.P., Spakman, W. and Wortel, R., 1995. Thermal structure of the continental lithosphere: constraints from seismic

tomography. *Tectonophysics*, *244*(1-3), pp.107-117.

Goes, S., Simons, F.J. and Yoshizawa, K., 2005. Seismic constraints on temperature of the Australian uppermost mantle. *Earth and Planetary Science Letters*, *236*(1), pp.227-237.

Goes, S. and van der Lee, S., 2002. Thermal structure of the North American uppermost mantle inferred from seismic tomography. *Journal of Geophysical Research: Solid Earth*, *107*(B3).

Goes, S., Govers, R. and Vacher, P., 2000. Shallow mantle temperatures under Europe from P and S wave tomography. *Journal of Geophysical Research: Solid Earth*, *105*(B5), pp.11153-11169.

Goutorbe, B., 2010. Combining seismically derived temperature with heat flow and bathymetry to constrain the thermal structure of oceanic lithosphere. *Earth and Planetary Science Letters*, *295*(3), pp.390-400.

Goutorbe, B. and Hillier, J.K., 2013. An integration to optimally constrain the thermal structure of oceanic lithosphere. *Journal of Geophysical Research: Solid Earth*, *118*(1), pp.432-446.

Hasterok, D., 2013. A heat flow based cooling model for tectonic plates. *Earth and Planetary Science Letters*, *361*, pp.34-43.

Hillier, J.K. and Watts, A.B., 2005. Relationship between depth and age in the North Pacific Ocean. *Journal of Geophysical Research: Solid Earth*, *110*(B2).

Hoggard, M.J., Winterbourne, J., Czarnota, K. and White, N., 2017. Oceanic residual depth measurements, the plate cooling model, and global dynamic topography. *Journal of Geophysical Research: Solid Earth*, *122*(3), pp.2328-2372.

Humphreys, E.D. and Dueker, K.G., 1994. Physical state of the western US upper mantle. *Journal of Geophysical Research: Solid Earth*, *99*(B5), pp.9635-9650.

Johnson, H.P. and Carlson, R.L., 1992. Variation of sea floor depth with age: a test of models based on drilling results. *Geophysical Research Letters*, *19*(19), pp.1971-1974.

Jordan, T.H., 1975. The continental tectosphere. *Reviews of Geophysics*, *13*(3), pp.1-12.

Kennett, B.L.N., 1995. Approximations for surface-wave propagation in laterally varying media. *Geophysical Journal International*, *122*(2), pp.470-478.

Kustowski, B., Ekström, G. and Dziewoński, A.M., 2008. Anisotropic shear-wave velocity structure of the Earth's mantle: A global model. *Journal of Geophysical Research: Solid Earth*, *113*(B6).

Lee, C.T.A., Lenardic, A., Cooper, C.M., Niu, F. and Levander, A., 2005. The role of chemical boundary layers in regulating the thickness of continental and oceanic thermal boundary layers. *Earth and Planetary Science Letters*, *230*(3), pp.379-395.

Lister, C.R.B., 1974. On the penetration of water into hot rock. *Geophysical Journal International*, *39*(3), pp.465-509.

McKenzie, D., Jackson, J. and Priestley, K., 2005. Thermal structure of oceanic and continental lithosphere. *Earth and Planetary Science Letters*, *233*(3), pp.337-349.

McKenzie, D.P., 1967. Some remarks on heat flow and gravity anomalies. *Journal of Geophysical Research*, *72*(24), pp.6261-6273.

Müller, R.D., Sdrolias, M., Gaina, C. and Roest, W.R., 2008. Age, spreading rates, and spreading asymmetry of the world's ocean crust. *Geochemistry, Geophysics, Geosystems*, *9*(4).

Parsons, B. and McKenzie, D., 1978. Mantle convection and the thermal structure of the plates. *J. geophys. Res*, *83*(B9), pp.4485-4496.

Parsons, B. and Sclater, J.G., 1977. An analysis of the variation of ocean floor bathymetry and heat flow with age. *Journal of geophysical research*, *82*(5), pp.803-827.

Perry, H.K.C., Jaupart, C., Mareschal, J.C. and Shapiro, N.M., 2006. Upper mantle velocity-temperature conversion and composition determined from seismic refraction and heat flow. *Journal of Geophysical Research: Solid Earth*, *111*(B7).

Priestley, K. and McKenzie, D., 2006. The thermal structure of the lithosphere from shear wave velocities. *Earth and Planetary Science Letters*, *244*(1), pp.285-301.

Renkin, M.L. and Sclater, J.G., 1988. Depth and age in the North Pacific. *Journal of Geophysical Research: Solid Earth*, *93*(B4), pp.2919-2935.

Ritzwoller, M.H., Shapiro, N.M. and Zhong, S.J., 2004. Cooling history of the Pacific lithosphere. *Earth and Planetary Science Letters*, *226*(1), pp.69-84.

Röhm, A.H., Snieder, R., Goes, S. and Trampert, J., 2000. Thermal structure of continental upper mantle inferred from S-wave velocity and surface heat flow. *Earth and Planetary Science Letters*, *181*(3), pp.395-407.

Romanowicz, B., 2009. The thickness of tectonic plates. *Science*, *324*(5926), pp.474-476.

Schaeffer, A.J. and Lebedev, S., 2013. Global shear speed structure of the upper mantle and transition zone. *Geophysical Journal International*, *194*(1), pp.417-449.

Schubert, G., Froidevaux, C. and Yuen, D.A., 1976. Oceanic lithosphere and asthenosphere: thermal and mechanical

structure. *Journal of Geophysical Research*, *81*(20), pp.3525-3540.

Shapiro, N.M. and Ritzwoller, M.H., 2002. Monte-Carlo inversion for a global shear-velocity model of the crust and upper mantle. *Geophysical Journal International*, *151*(1), pp.88-105.

Sleep, N.H., 2005. Evolution of the continental lithosphere. *Annu. Rev. Earth Planet. Sci.*, *33*, pp.369-393.

Sleep, N.H., 1971. Thermal effects of the formation of Atlantic continental margins by continental break up. *Geophysical Journal International*, *24*(4), pp.325-350.

Stein, C. A., and Stein, S., 1992. A model for the global variation in oceanic depth and heat flow with lithospheric age. *Nature*, *359*(1).

Stein, S. and Wysession, M., 2009. *An introduction to seismology, earthquakes, and earth structure*. John Wiley & Sons.

Turcotte, D.L. and Oxburgh, E.R., 1967. Finite amplitude convective cells and continental drift. *Journal of Fluid Mechanics*, *28*(01), pp.29-42.

Turcotte, D.L. and Schubert, G., 2002. Geodynamics, Cambridge University Press. *New York*, pp.164-165.

Wegener, A., 1966. *The origin of continents and oceans*. Courier Corporation.

Yan, B., Graham, E.K. and Furlong, K.P., 1989. Lateral variations in upper mantle thermal structure inferred from three-dimensional seismic inversion models. *Geophysical Research Letters*, *16*(5), pp.449-452.

Zhang, Y.S. and Lay, T., 1999. Evolution of oceanic upper mantle structure. *Physics of the earth and planetary interiors*, *114*(1), pp.71-80.